journal

*J. Am. Ceram. Soc.*, **84** [4] 685–92 (2001)

# Influence of Plasma Spray Parameters on In-Flight Characteristics of $ZrO_2$–8 wt% $Y_2O_3$ Ceramic Particles

Ahmet Kucuk,*,† Rogerio S. Lima, and Christopher C. Berndt*

Center for Thermal Spray Research, Department of Materials Science and Engineering, The State University of New York at Stony Brook, Stony Brook, New York 11794

**Yttria-partially-stabilized zirconia was atmospherically plasma sprayed by systematically varying the process conditions including carrier gas flow rate, torch power, standoff distance, and $Ar/H_2$ ratio in the plasma gas mixture. The in-flight particle parameters such as temperature, velocity, number, and size were determined using a commercially available diagnostic system. The particle parameters were controlled by the particle trajectory in the plume and plasma jet characteristics. The average temperature and the velocity of particles, which reached their maximum at an intermediate carrier gas flow rate of 3.5 L/min, varied as much as 6% and 25%, respectively, with a 75% variation in the carrier gas flow rate by going from the lowest to the intermediate rates. The average temperature and the velocity of particles were lower for a lower torch power, a higher $Ar/H_2$ ratio, and a larger standoff distance. It was necessary to obtain data on particle populations larger than 1000 for statistically reliable and reproducible information from the diagnostic system.**

## I. Introduction

THERMAL spray technology has been used to produce ceramic, metal, and plastic coatings for various applications such as wear resistance, high-temperature insulation, and corrosion protection.[1] Yttria-partially-stabilized zirconia (YSZ) coatings with an intermediate metal bond coat layer on super alloys have been widely used as thermal barrier coatings in aerospace applications.[1] It has been reported that the performance of thermally sprayed coatings is strongly controlled by the process parameters.[2,3] Therefore, more complete understanding of the process would allow the manufacture of coatings with improved performance. It is crucial to understand *in situ* process factors and the manner in which deposits form from individual units (i.e., splats) and produce coatings with varied, anisotropic properties. Especially, the deposition efficiency, which is the percentage of particles deposited on the substrate within an ensemble of particles arriving at the substrate, needs to be examined since this quantity is directly related to coating realization (i.e., zero deposition efficiency implies that no coating is achieved) and it strongly depends on the in-flight particle characteristics.

Various process diagnostic systems have been used in the field of thermal spray technology: in-flight diagnostic sensors,[4–6] acoustic emission transducers,[7,8] high-speed CCD cameras,[9,10] and pyrometers.[11,12] In these systems, a two-color pyrometer is used to determine the temperature of in-flight particles, and laser Doppler velocimetry (LDV) and laser two-focus systems (L2F) are used to determine the velocity of in-flight particles. High-speed CCD cameras have gained the most support in the thermal spray field to determine particle size and distribution.[6,9,10] In addition, there exist commercially available in-flight systems that allow simultaneous measurements of the particle characteristics.[4,13] One of these systems, the Tecnar DPV2000 in-flight diagnostic system (Tecnar Automation, St. Hubert, Quebec, Canada), which combines two-color pyrometry and an L2F system to provide temperature, velocity, particle size, and distribution, has been used by many researchers.[4,7,14–17]

In the current study, the in-flight particle properties such as temperature, velocity, and size of yttria-partially-stabilized zirconia (YSZ) during plasma spraying will be examined to understand the influence of the process parameters on these properties. The plasma spray parameters including carrier gas flow rate, torch power, $Ar/H_2$ ratio, and standoff distance are systematically varied. A special emphases on the carrier gas flow rate is given since no such systematic detailed study on the carrier gas flow rate is found in the open literature even though the influence of torch power, $Ar/H_2$ ratio, and standoff distance on the characteristics of YSZ coatings is well documented and also intuitively predictable.

## II. Experimental Procedure

### *(1) Spraying Conditions*

Yttria-partially-stabilized (8%) zirconia was plasma sprayed without restriction into an open, ambient enviroment using a Metco 3MB plasma torch with a Metco GH nozzle (Sulzer Metco, Westbury, NY-USA) mounted on a six-axis articulated robot (Model S400, GMF Fanuc, Charlotteville, VI-USA). The commercially available Metco HOSP™ (hot oven spherical powder) 204NS-AE7590 (Sulzer-Metco, Westbury, NY) powder with an average particle size of 80 μm (−110 + 10 μm) was used as feedstock. The powder had hollow sphere morphology with a smooth surface resulting from the spray drying followed by an oven or flame densification process. A mechanical feeder was used

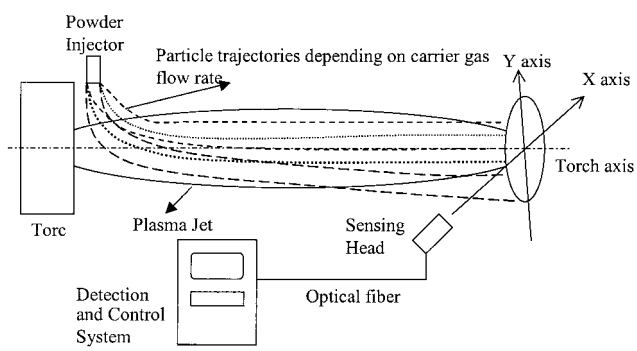


**Fig. 1.** Schematic diagram of the plasma spray and in-flight diagnostic systems. Note that the carrier gas flow rate changes the particle trajectory.

R. W. Rice—contributing editor

Manuscript No. 188681. Received March 27, 2000; approved November 10, 2000.
Two of the authors (A.K. and C.C.B.) gratefully acknowledge financial support from the National Science Foundation under NSF-MRSEC DNR, Grant No. 9632570. One of the authors (R.S.L.) would like to acknowledge financial support from ONR Grant No. N00014-97-0843.

*Member, American Ceramic Society.
†Present address: Karl Storz Endovision, Inc., Charlton, Massachusetts 01507.

**Table I. Spray Parameters**

| Parameters | S-1 | S-2 | S-3 | S-4 | S-5 | S-6 |
|---|---|---|---|---|---|---|
| Current (A) | 600 | 600 | 600 | 600 | 600 | 600 |
| Voltage (V) | 70 | 70 | 70 | 70 | 70 | 55 |
| Primary gas, Ar (L/min) | 40 | 40 | 40 | 40 | 50 | 50 |
| Secondary gas, $H_2$ (L/min) | 12 | 12 | 12 | 12 | 11 | 4.1 |
| Powder carrier gas, Ar (L/min) | 2.0 | 4.0 | 6.0 | 3.5 | 3.5 | 3.5 |
| Standoff distance (mm) | 80 | 80 | 80 | 80 | 100 | 100 |
| Feeding rate (g/min) | 2 | 2 | 2 | 2 | 2 | 2 |

to introduce the powders at a rate of 2 g/min into the plasma jet through a Metco No. 2 powder injector, which was vertically located 9 mm from the torch axis, and 7 mm from the torch exit (Fig. 1).

Spray parameters are listed in Table I. As can be seen, the carrier gas flow rate was systematically changed from 2.0 to 3.5 L/min (S-1–S-4) to investigate the influence of particle trajectory in the plasma jet on its in-flight particle characteristics. Spray parameters S-4, S-5, and S-6, all of which are often used in our day-to-day plasma spray practice, were selected to investigate the influence of standoff distance along with torch power and $Ar/H_2$ ratio.

### *(2) In-Flight Particle Diagnostics*

The particle temperature, velocity, and size in the plasma jet were measured using a Tecnar DPV-2000 system (Tecnar Automation, St. Hubert, Quebec, Canada). The system has been described in detail elsewhere.[4,13,19] Briefly, the system consists of a tubular sensing head linked to a detection box with light detectors through an optical fiber bundle and an IBM compatible PC. The system monitors individual particles in the plasma plume to provide temperature, velocity, and size information. The temperature is measured from the radiation intensities at two different wavelengths. The velocity is determined via a two-slit mask covering the front face of the sensing head (Fig. 1). The particle size can be estimated from the radiation intensities for a particle with known emissivity. In the current study, a normalized particle size rather than the absolute value will be reported, as will be explained below. The particle temperature and velocity were determined at the center line of the plume, where the particle flow density was the highest, as well as at various other locations throughout the plume at a constant sensor–plasma torch distance. The measurements at the center lines were conducted for 30 to 120 s depending on the number of particles monitored. Each position in the cross-sectional scans was monitored for 5 s with an interval of 5 mm at 25 different positions with the center line being the origin of the cross section.

## III. Results

### *(1) Center-Line Values*

*(A) Temperature:* Figure 2 illustrates the temperature distribution at the center line of the plume for the particles sprayed under various spray parameters. The average particle temperatures at the center line are statistically different for the groups sprayed at different processing conditions except for those of groups S-2 and S-3. The average temperature decreases in the following order: S-4 > S-2 = S-3 > S-1 > S-5 > S-6 as proved by a Student's *t*-test. The variation in the temperature of particles at the center line is similar for different groups (around ±13%). The average temperature at the center line first increases with the increasing carrier gas flow rate, then decreases with further increase in the carrier gas flow rate for a given standoff distance (S.D.) of 80 mm (Fig. 3).

The proportion of molten particles can be calculated from the temperature distribution by knowing that the melting point of 8 wt% $Y_2O_3$ partially stabilized zirconia is 2700°C. The percentage of molten particles within the total particle population that reaches the designated standoff distance (Table I) changes by 19%, 33%, 30%, 35%, 11%, 3% for the groups S-1 to S-6, respectively. One should notice here that the temperature values represent the temperature at the surface or near the surface of the particles; i.e., the inner part of the particles may have lower temperature. Therefore, the values given above should be taken as the percentage of molten or semimolten particles rather than the percentage of completely molten particles.

*(B) Velocity:* Figure 4 illustrates the velocity distribution of particles at center lines sprayed with different process parameters. As shown in Fig. 4, part of the distribution is labeled as a "phantom peak" that is an unavoidable artifact resulting from the instrument.[4,13] The phantom peak represents two identical out-of-focus particles crossing the measurement volume with such a time shift that they appear to be a symmetrical, lower-velocity particle. It was suggested by the manufacturer that the "phantom peak" does not contain accurate information and should be discarded from the data.[13] The average velocity values listed in the plots are calculated by discarding the "phantom peak." The average velocity first increases, then decreases with increasing carrier gas flow rate (Fig. 3). In addition, lower torch power or longer standoff distance results in lower particle velocities.

*(C) Particle Size:* Since the emissivity of the particles was not known, the particle size determined from the temperature measurement was calibrated with respect to the average particle size of the starting powder. The average in-flight particle sizes were determined to be 80 ± 34, 80 ± 40, 80 ± 42, 80 ± 49, 80 ± 38, and 80 ± 33 μm for samples S-1 to S-6, respectively. As can be seen, the coefficient of variation (CV) for the particle size in different groups is slightly different; i.e., CV varies from 41% to 61% for groups S-6 and S-4, respectively. This behavior indicates a change in the process characteristics. For the S-4 condition, for instance, the chance of particles of wide size distribution in reaching the substrate is higher than that of particles sprayed under S-6 conditions. As a result, a narrower splat size distribution might be expected for coatings sprayed under the S-6 conditions. Since the information generated from the diagnostic system on the particle size is limited, the particle size and distribution will not be discussed further.

*(D) Number of Particles:* Figure 3 illustrates the average number of particles monitored per second through the center-line position. The average particle rate first increases and then decreases with increasing carrier gas flow rate in the center-line position. In addition, the rate drops for a longer standoff distance and a lower torch power.

### *(2) Various Positions in the Plume Cross Section*

*(A) Temperature:* The temperature distribution through the plume cross section (*X*–*Y*) for a constant standoff distance (either 80 or 100 mm as given in Table I) is illustrated in Fig. 5. As shown, the temperature distribution significantly changes depending on the spray conditions. In general, the distributions do not show any symmetry. This agrees with the theory of the plasma spray process[20] and the earlier measurements reported.[12,20,21] The distributions are asymmetric with respect to the $Y = 0$ ($X$-axis), implying that the injection port alignment does not provide perfect symmetry. As seen in Fig. 5, the distribution data were not presented for some locations (e.g., $Y = -10$ for S-1) because the

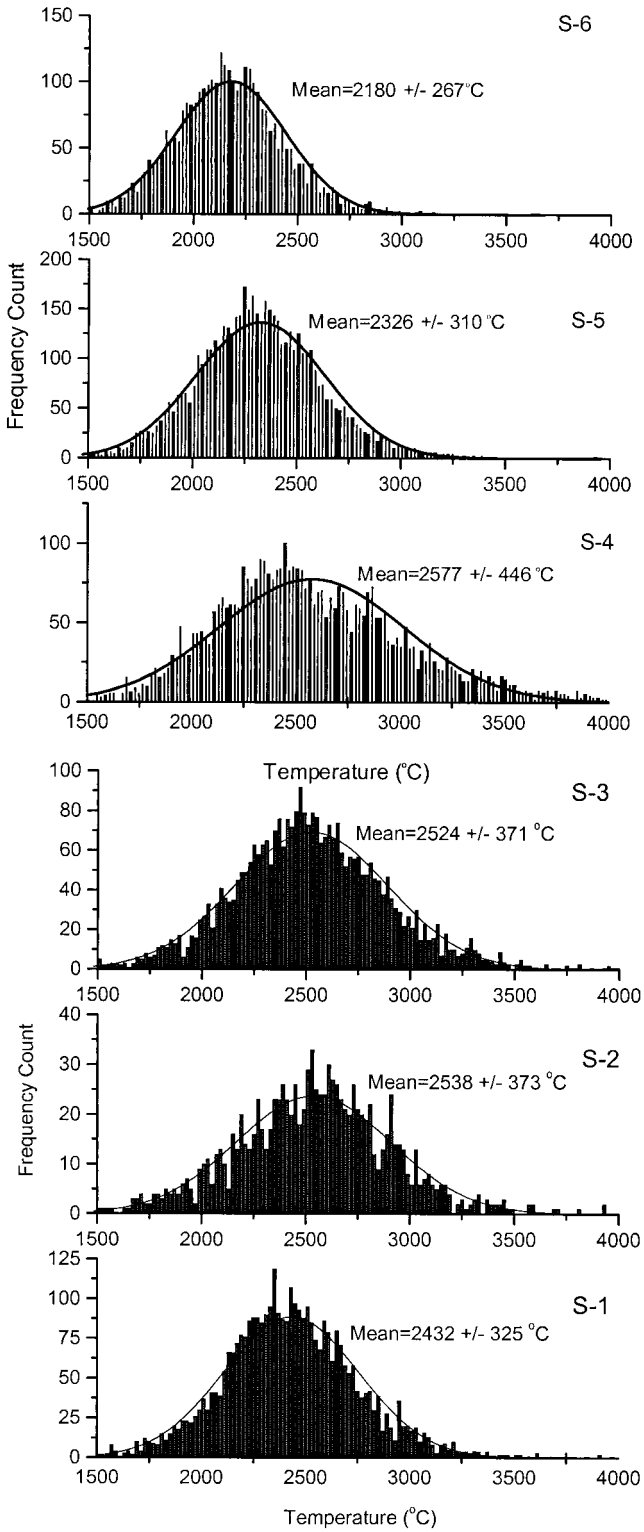


**Fig. 2.** Temperature distribution at the center lines, where the particle flow density is the highest, for different process conditions listed in Table I. Note that sample size is 1.

number of particles monitored at the mentioned location was too low (less than 50) to provide statistically reliable information. In addition, a temperature distribution analysis for some locations was avoided because of poor statistical reliability. Therefore, the average temperature for each location was used rather than a distribution.

Depending on the carrier gas flow rate, the particles at the center-line position lie above, at, or below the hottest zone of the plume for parameter set S-1, S-2, and S-3, respectively, for

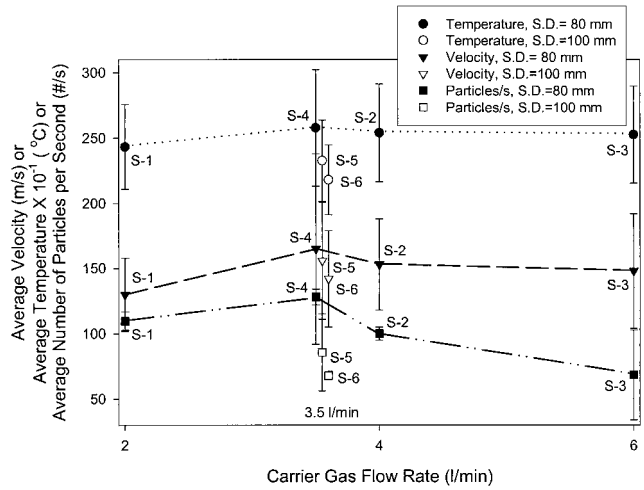


**Fig. 3.** Change of the particle in-flight average temperature, velocity, and the number at the center line with increasing carrier gas flow rate.

increased carrier gas flow. Similarly, the hottest zone shifted to the left with respect to the $Y = 0$ plane ($X$-axis) with increasing carrier gas flow rate and indicated off-axis alignment of the injector port; i.e., the injector port was installed off center and to the right of the $X$-axis. A carrier gas flow rate of 3.5 to 4.0 L/min provided a center-line position at the hottest zone of the plume. The hottest zone of the plume moved away from the center line with decreasing torch power for a constant carrier gas flow rate (Fig. 5(f)).

*(B) Velocity:* The distribution of the average velocity values throughout the cross section of the plume for a given standoff distance was not obtained reliably because the "phantom peak" could not have been discarded from the data since the number of data points for a given location was too low for statistical analysis.

## IV. Discussion

### *(1) Diagnostic Tool*

Even though the Tecnar-DPV2000 is a strong *in situ* diagnostic tool, one should be cautious with the data obtained from the measurements. The measurements, in common with similar experimental techniques, need to be conducted on a large sample group size; i.e., the number of particles from which information collected should be as large as possible to provide higher accuracy and reliability. This can be achieved by increasing the measurement time. The measurement time varied from 30 to 120 s for the center-line measurements, allowing 1000 to 5000 particle counts. However, the measurement time was 5 s to collect information at individual locations during the mapping of the plume cross-section characteristics. This measurement time allowed particle counts of 1 to 800. In the data analysis for the mapping study, data representing fewer than 50 particle counts were discarded. Temperature values are reliable and reproducible for data collected from a large sampling size. However, caution must be exercised when examining the velocity data since corrections concerning the "phantom peak" can be taken into account only when the sample size is large.

### *(2) Penetration of Particles into the Plasma Jet*

When externally injected gas–powder mixtures interact with the plasma jet, the heat exchange between cold particle–gas mixtures and the hot plasma jet changes the temperature distribution of both the particles and plasma jet.[12] The manner and duration of this interaction depends on the particle momentum[11,22] and plasma jet properties including torch power, plasma gas composition,[19,23] and nozzle diameter for a given plasma torch. The particle momentum ($vm$, where $v$ is the velocity and $m$ is the mass) mostly depends on the carrier gas flow rate. A particle can either (i) bounce off from the plasma flow, (ii) penetrate into the plasma jet and flow with it,

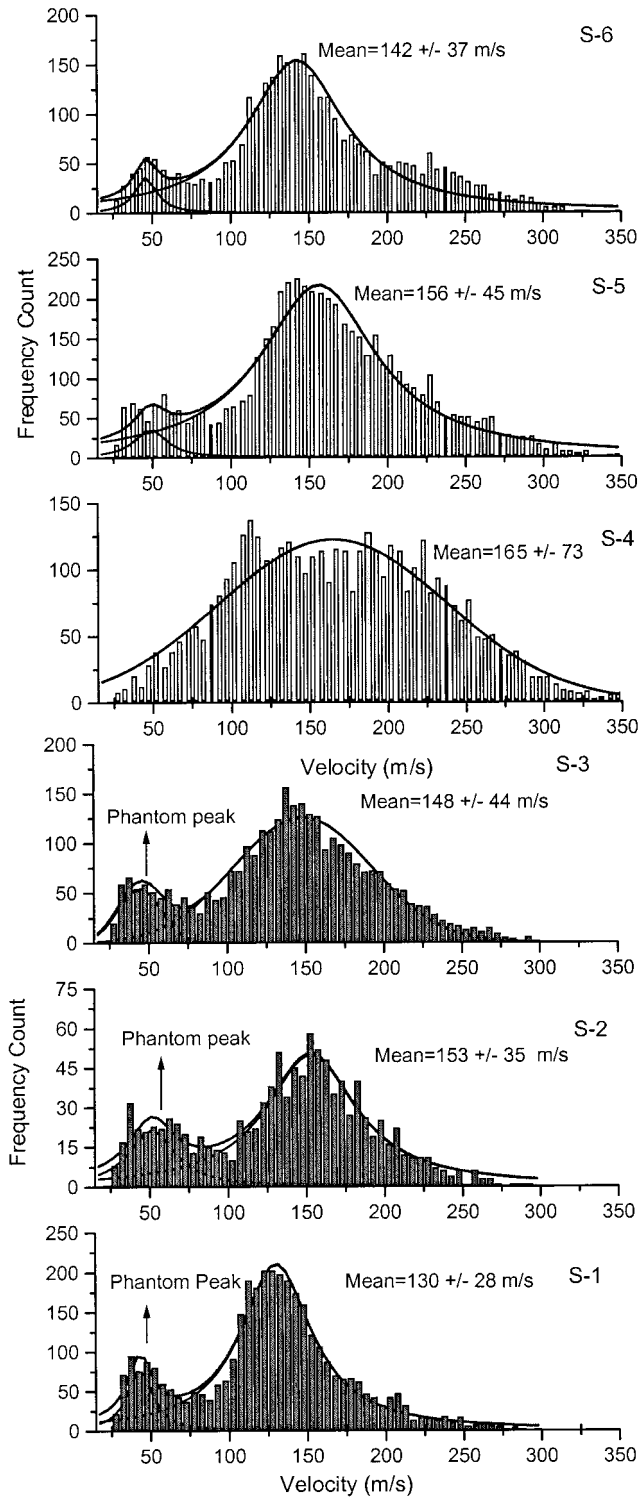


**Fig. 4.** Velocity distribution at the center lines, where the particle flow density is the highest, for different process conditions listed in Table I. Note that sample size is 1.

or (iii) penetrate into the plasma jet and cross over the plasma jet, depending on the momentum being low, medium, and high, respectively. The particle injection velocity of the Sulzer Metco 204NS YSZ powder loaded with a rate of 20 g/min and 3.0 to 6.0 L/min carrier gas flow through a standard Sulzer Metco injector (with 2.8 mm inner diameter and 1.8 mm exit diameter) using a Miller Model 1270 powder feeder was reported as $9 \pm 1.5$ to $14.5 \pm 3$ m/s.[22,24] It was also found that the particle injection velocity of the same powder did not show any particle size dependence.[24] Vardelle *et al.*[11,25] reported that the injection velocities of fused and crushed alumina particles with $-21 + 15$ μm and $-90 + 45$ μm sizes were $47.9 \pm 14.4$ and $12.7 \pm 2.3$ m/s injected through a 1.6 mm inner diameter injector with carrier gas flow rates of 7.5 and 2.5 L/min, respectively.

The difference in the particle injection velocities reported in Vardelle's[11,25] study was most likely the result of the difference in the carrier gas flow rate. Assuming that YSZ and alumina powders[‡] behave similarly, the particle injection values from Fincke *et al.*[24] and Vardelle[25] would be in agreement when one takes into consideration that the injector diameters are different. For further evolution in the current study, values from Fincke *et al.* were used since the process parameters were most similar to those of the current study.

Vardelle *et al.*[12] derived the following equation to calculate the penetration of particles into a plasma jet:

$$y = v_0\left(\frac{\rho_p d_p^2}{18\eta_g}\right)\left\{1 - \exp\left[-\left(\frac{18\eta_g}{\rho_p d_p^2}\right)t\right]\right\} \quad (1)$$

where $y$ is the vertical (parallel to injection axis) injection distance traveled by the particle (p) with a diameter of $d_p$ and density of $\rho_p$, $v_0$ is the initial particle injection velocity, $\eta_g$ is the viscosity of the plasma jet gas, and $t$ is the residence time in the plume. One can find that the residence time is 0.5–1 ms by taking an average particle velocity (in the plasma jet direction) of 100–200 m/s and a standoff distance of 8–10 mm. The viscosity of the plasma jet consisting of 20% $H_2$–80% Ar gas mixture was reported to vary from $0.1 \times 10^{-3}$ to $0.25 \times 10^{-3}$ Pa·s in the temperature range of 5000 to 15 000 K with a maximum at 10 000 K.[26] The vertical distances traveled, $y$ values, calculated from Eq. (1) for various process parameters are given in Fig. 6. The $y$ values for particles larger than 35 μm do not significantly change for a given spray condition. The carrier gas flow and residence time (in turn, the particle velocity in the plume and the standoff distance) drastically influences the $y$ value; i.e., a 100% increase in carrier gas flow rate increases the $y$ value by almost 100%. Therefore, it would be expected that the particle trajectories for various process parameters in the current study might significantly differ.

One also needs to consider the influences of a cold gas–solid mixed stream on a hot plasma stream when these two streams flow in perpendicular directions. Vardelle *et al.*[12] reported that the plasma jet axis shifted by 2° with respect to the torch axis toward the direction of the injection when an external injection system was used in a process where 27 L/min Ar + 7 L/min $H_2$ plasma gas mixtures and 8 L/min Ar carrier gas with a 1.6 mm injector were used. Similarly, Chivel *et al.*[21] found a 2.8° shift for an atmosphere plasma spray process. Therefore, the plasma jet axis shifts 3–5 mm with respect to the torch axis at a standoff distance of 80 to 100 mm as in the current study when an external injection is used.

As a result, the temperature and velocity distributions of the particles reported above need to be analyzed by taking these two aforementioned characteristics into account, namely, the particle and plasma jet trajectories.

### *(3) Influence of Spray Conditions on Particle Temperature*

As given in Fig. 3, the change of center-line average particle characteristics such as temperature and velocity exhibit a maximum with respect to change in the carrier gas flow rate. This suggests that a carrier gas flow rate of 3.5 L/min is an ideal value that achieves the best spray performance in the given system. It is most likely that the particle flux center line and the plasma jet axis coincide at this carrier gas flow rate. The particles injected with a carrier gas flow rate less than 3.5 L/min penetrate into the plasma jet to a certain extent, i.e., in such a way that they do not reach the plasma jet axis, but reside in the cooler zone of the plasma jet before reaching the substrate. On the other hand, the particles that

[‡]Metco 204NS is a hollow spherical YSZ powder with a density of 4 g/cm$^3$ while the alumina powder also has a density of around 4.0 g/cm$^3$.

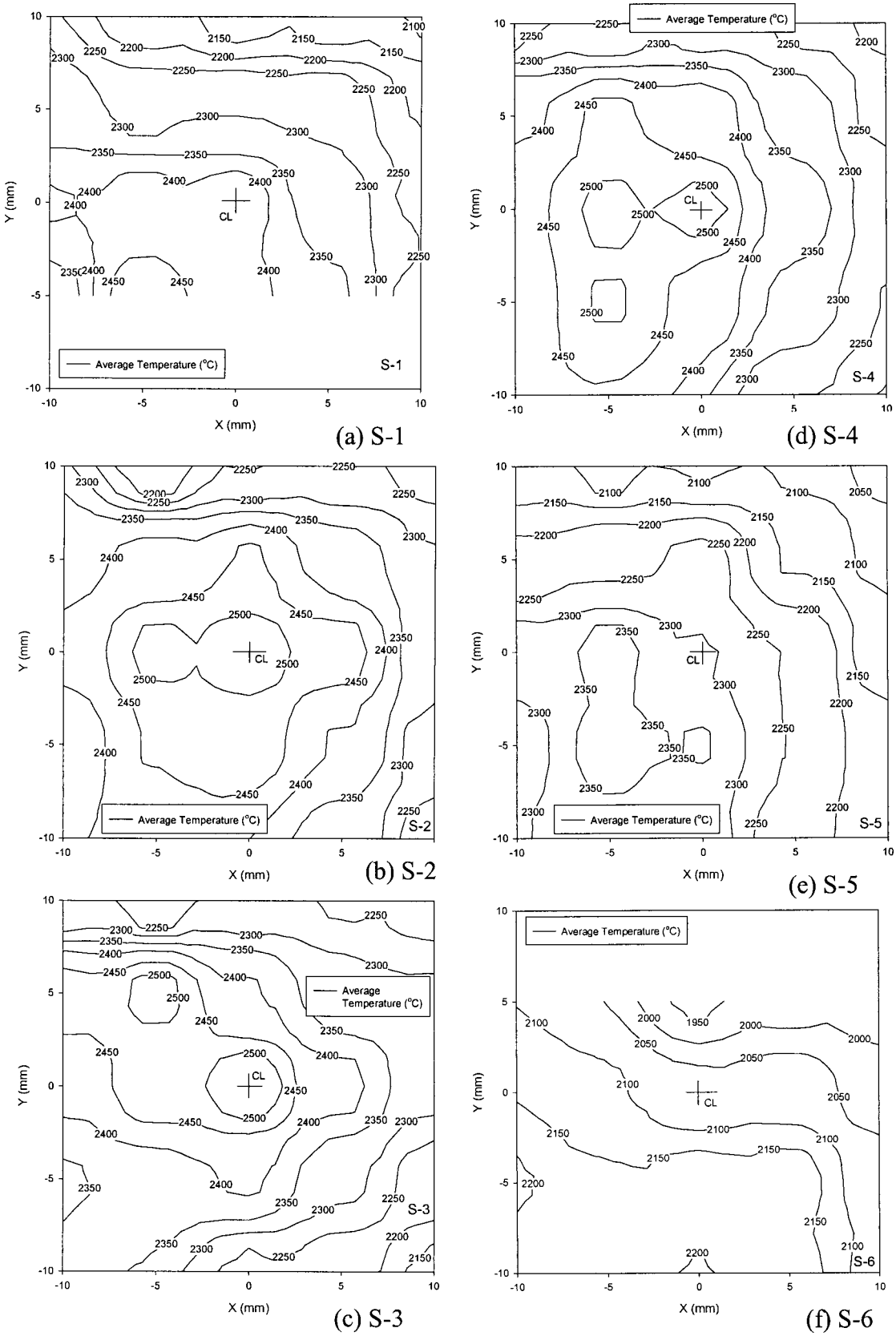


**Fig. 5.** Average particle temperature distribution throughout the cross section of the plum for plasma spray conditions: (a) S-1, (b) S-2, (c) S-3, (d) S-4, (e) S-5, and (f) S-6. The origin (0,0) represents the center line (CL) where the particle flow density is the highest. The axes *X* and *Y* are as described in Fig. 1.

are injected with carrier gas flow rates higher than 3.5 L/min penetrate into the plasma sufficiently to reach the plasma jet axis and reside at a location which is lower than the axis where the temperature is lower than the core temperature. This observation can be easily seen in Fig. 5, where the temperature distributions throughout the plasma jet cross section are given. As presented in Figs. 5(a) and (c), the center line for sample S-1, which has a carrier gas flow rate of 2.0 L/min, is located above the plasma jet axis, where temperature is the highest, while the center line for sample S-3, which has a carrier gas flow rate of 6.0 L/min, lies

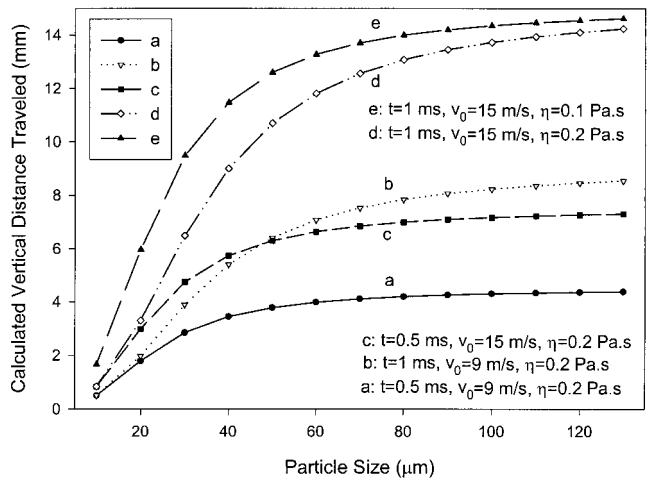


**Fig. 6.** Change of calculated vertical distance traveled by an injected particle into plasma jet with the spray parameters.

below the plasma jet axis. The center-line positions of samples S-1 and S-3 are about 8–10 mm apart from each other, which is in agreement with the calculated values in Fig. 6. As mentioned earlier, there is also a shift of the plasma jet axis to slightly left (about 5 mm) of the center line. This shift arises from the installation of the powder injector; i.e., the injector axis is either slightly on the right of the torch axis or not perfectly perpendicular to the torch. The shift, being similar for all of the samples, suggests that the degree of misalignment is small.

When the influences of torch power levels are compared (S-5 vs S-6), it can be seen that the center-line temperature drops significantly by 150°C at the lower power (Fig. 4). In addition, the center-line positions with respect to plasma jet axis for samples S-5 and S-6 exhibit different behavior than sample S-4, showing that all three had the same carrier gas flow, but S-4 was at 80 mm standoff distance with a higher torch power. Both of the center-line positions for samples S-5 and S-6 are located above the plasma jet axis (Figs. 5(e) and (f)). One would expect that the center line and the plasma jet axis would be closer since the residence time is longer for the standoff distance of 100 mm (see Fig. 6 for the influence of the residence time on the particle trajectory). However, the change in the properties of the plasma jet must also be considered. A lower $H_2$ content in plasma mixtures increases the viscosity of the plasma,[23] and in turn, the vertical distance traveled by particles into the plasma jet decreases (see Fig. 6).

### *(4) Influence of Spray Conditions on Particle Velocity*

When a particle moving vertically to a torch axis encounters the plasma jet, its vertical velocity decelerates to zero while its horizontal (parallel to spray direction) velocity accelerates. The final velocity of a particle at a given standoff distance is controlled by the velocity of the plasma jet and the particle trajectory. It was reported in earlier studies[19,20,26] that the plasma jet velocity is higher near the plasma jet axis and the plasma torch exit. Therefore, it is no surprise that sample S-4, whose center line is right at the plasma axis, has the highest average particle velocity at its center line. Similarly, the average center-line velocities of samples S-1, S-2, and S-3 vary depending on the center-line position with respect to the plasma jet axis; i.e., the closer the plasma jet axis, the higher the velocity. As mentioned above, the center line of sample S-1 locates above the plasma jet axis while the center line of sample S-3 lies below the plasma jet axis. The reasons for the velocity of sample S-3 being higher than that of sample S-1 are the following: (i) the S-3 particles pass through the plasma jet axis where the velocity is the highest before reaching a standoff distance of 80 mm, and (ii) the S-3 center-line position is slightly closer to the plasma jet axis than the S-1 center line.

Sample S-5 has a high center-line average velocity when compared with samples S-1 and S-3 (Fig. 4) although it has a lower $Ar/H_2$ ratio in the plasma. It was reported that addition of $H_2$ to Ar increases the velocity of the plasma jet for a given power level.[23] The high velocity for sample S-5 could be because the residence time for sample S-5 is longer due to the standoff distance being 100 mm. A longer residence time allows further time for acceleration of particles in the plasma jet. Similarly, S-6 has a comparably high velocity for the same reason.

### *(5) Comparison with Previous Data*

Although no *in situ* diagnostic study information on air plasma spraying of 8%-$Y_2O_3$-partially-stabilized zirconia using a Metco 3MB torch was found in the open literature, it is still valuable to compare the results reported for various APS torches in the open literature to the results in the current study. The results from previous studies concerning the atmospheric spraying of yttria-partially-stabilized zirconia are summarized in Table II. In the table, the maximum average temperature and velocity values are included along with the spray conditions and equipment, and the measurement technique whenever possible. The spray conditions included are, in the order presented, torch current and voltage, primary and secondary gas flow rates, injector type, carrier gas flow rate, powder feed rate, and average particle size depending on the available information. The spray conditions listed in Table II cover the range of values for commonly used process parameters

**Table II. Comparison of In-Flight Characteristics for Plasma-Sprayed YSZ Particles Using Various Techniques†**

| *T* (°C) | *v* (m/s) | Torch | Conditions | SD (mm) | Method | Ref. |
|---|---|---|---|---|---|---|
| 2600–3000 | 200 | Miller SG100 | 900 A, 34 V, 47 Ar + 22.2 He L/min, 6.1 L/min Ar, 40 μm | 50–120 | LDV, TCP | 27 |
| 2500 | | PTF4 | 600 A, 58 V, 32 Ar + 12 $H_2$ L/min, 5 g/min, 40 μm | 120 | LV, TCP | 28 |
| 2350 | 300 | PTF4 | 630 A, 41 + 14 $H_2$ L/min, 2.5 Ar, −45 + 22 μm | 120 | LDA | 23 |
| 2800 | 160 | Metco 9MB | 600 A, 75 V, 40 Ar + 12 $H_2$ L/min, 5.0 Ar, 20 g/min, 30 μm | 100 | PDPA | 24 |
| 2800 | 180 | Miller SG100 | 800 A, 34–42 V, 50 Ar + 2 $H_2$ L/min, 6.5 L/min Ar, 23 g/min, −45 + 22 μm | 63 | Tecnar | 14 |
| 2900 | 160 | Metco F4-MB | 605 A, 70 V, 37 Ar + 12 $H_2$ L/min, 1.3 L/min Ar, 35 g/min, −45 + 22 μm | 140 | Tecnar | 15 |
| 3000 | 130 | Metco F4-MB | 475 A, 66 V, 42 Ar + 9 $H_2$ L/min, 1.3 L/min Ar, 35 g/min, −45 + 22 μm | 140 | Tecnar | 15 |
| 2600 | 150 | Metco SM-F100 | 450 A, 41 V, 42 Ar + 4 $H_2$ L/min, 2.5 L/min Ar, 35 g/min, −45 + 22 μm | 70 | Tecnar | 15 |
| 2750 | 100 | Metco SM-F100 | 350 A, 38 V, 42 Ar + 2 $H_2$ L/min, 2.5 L/min Ar, 35 g/min, −45 + 22 μm | 70 | Tecnar | 15 |
| 2400 | 160 | Metco 9MB | 600 A, 60 V, 39 Ar + 10 $H_2$ L/min, M-GH, 5 L/min $N_2$, 45 g/min, 80 μm | 102 | PDPA, TCP | 5 |
| 2600 | 250 | Metco 9MB | 600 A, 60 V, 58 Ar + ? $H_2$, Metco GP, 7 L/min $N_2$, 45 g/min, 80 μm | 76 | PDPA, TCP | 5 |
| 2100–2500 | 130–165 | Metco 3MB | Table I | 80–100 | Tecnar | This |

†See the text for details of the method and the conditions.

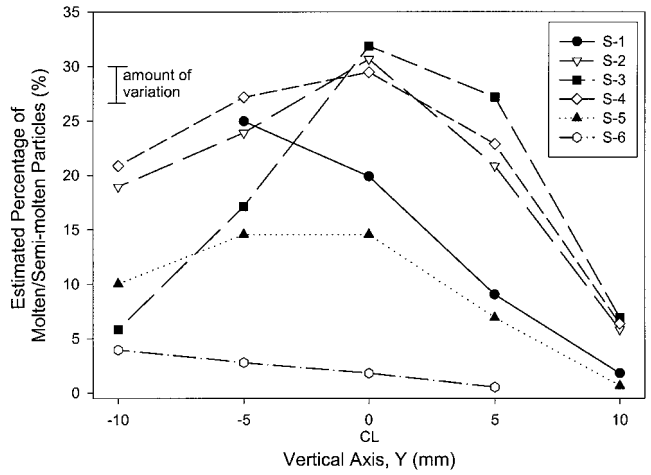


**Fig. 7.** Change of estimated percentage of molten and/or semimolten particles with vertical axis *Y*.

in the air plasma spraying of YSZ. The common standoff distance varies from 70 to 120 mm and the influence of the standoff distance on the particle characteristics has been extensively studied.[5,15,27]

The common techniques used include laser Doppler velocimeter (LVD), laser velocimeter (LV), phase Doppler particle anemometer (PDPA), two-color pyrometer (TCP), and the Tecnar DPV-2000 diagnostic system (Tecnar) which is the combination of a TCP and L2F. The torches studied are from three companies: Sulzer Metco (Westbury, NY), TAFA (currently part of Praxiar, Appleton, WI), and PlasmaTecnik (currently part of Sulzer Metco, Switzerland). The diagnostic values in the current study are in good agreement with the previous studies within the variation of the systems (Table II).

### *(6) Deposition Efficiency*

As mentioned in Section 3(1)(A), the percentage of particles that have a center-line average temperature higher than the melting point of the YSZ varies with the spray conditions. The percentage of particles increases from 19% for S-1% to 35% for S-4 and then decreases to 30% for S-3 within the particles whose temperature monitored at the center-line position. It should be noted that the carrier gas flow rate increased in the same order. In addition, the percentage dropped to as low as 3% for S-6, where the standoff distance and the torch power were large and low, respectively. Therefore, one would expect that deposition efficiencies for different carrier gas flow rates or torch power levels would differ.

In Fig. 7, the estimated percentage of molten and/or semimolten particles is given with respect to the vertical axis (*Y* axis). These percentages were calculated using the average temperature counters presented in Fig. 5 for the different spray conditions by taking the melting temperature of YSZ as 2700°C. The highest average temperature at a given vertical axis value was taken for the calculations. The percentage of particles that had temperatures higher than 2700°C was calculated by assuming that the particle temperature distribution is a normal distribution for a known average temperature. The estimated percentages in Fig. 7 were similar for samples S-2, S-3, and S-4. They differ drastically for samples S-5 and S-6. These percentages can be related to deposition efficiency at a given location in a deposit. The influence of spray parameters on the deposition efficiency and microstructure of the coating as well as relations between deposition efficiency and the in-flight particle characteristics are discussed elsewhere.[18]

## V. Conclusions

The in-flight characteristics of yttria-partially-stabilized zirconia particles were determined using a commercially available diagnostic system and were in good agreement with studies reported in the open literature. The temperature, velocity, number, and size of particles were measured in-flight for varying plasma spray conditions. It was found that the carrier gas flow rate significantly influences the in-flight particle properties since it determines the trajectory of a particle injected into a plasma jet. The particle trajectories were located above, at, or below the plasma jet axis depending on the carrier gas flow rate. The temperature and the velocity of particles close to the plasma jet axis were high owing to the fact that the plasma jet had a temperature and velocity distribution with the maximum in the axis and near the torch exit. A flow rate of 3.5 L/min optimizes the particle trajectory, for the studied torch characteristics, to provide high particle flow density at the highest temperature and velocity zone of the plasma jet. In addition to carrier gas flow rate, the plasma power, the $Ar/H_2$ ratio in plasma gas mixtures, and the standoff distance were also found to be influential on temperature and the velocity of particles. Lower torch power and longer standoff distance lower particle temperatures. The results regarding the torch power, the $Ar/H_2$ ratio, and the standoff distance were in good agreement with the previous extensive studies in the field.

The particle in-flight characteristics were also analyzed at various positions of the plume cross section for a given standoff distance. Temperature decreased on increasing the distance from the plasma jet axis. In general, a large particle number population is required to obtain statistically reliable and reproducible results from the measurement system and this is especially true for the velocity data.

## Acknowledgments

We appreciate the help from Steven Depola and Jon Gutleber of SUNY–Stony Brook in some of the in-flight measurements.

## References

[1]L. Pawlowski, *The Science and Engineering of Thermal Spray Coating*. Wiley, New York, 1995.

[2]A. Kucuk, C. C. Berndt, U. Senturk, R. S. Lima, and C. R. C. Lima, "Influence of Plasma Spray Parameters on Mechanical Properties of Yttria Stabilized Zirconia Coatings, I: Four Point Bend Test," *Mater. Sci. Eng.*, **284**, 29–40 (2000).

[3]A. Kucuk, C. C. Berndt, U. Senturk, and R. S. Lima, "Influence of Plasma Spray Parameters on Mechanical Properties of Yttria Stabilized Zirconia Coatings, II: Acoustic Emission," *Mater. Sci. Eng.*, **A284**, 41–50 (2000).

[4]J. Blain, F. Nadeau, L. Pouliot, C. Moreau, P. Gougeon, and L. Leblanc, "Integrated Infrared Sensor System for On Line Monitoring of Thermally Sprayed Particles," *Surf. Eng.*, **13** [5] 420–24 (1997).

[5]B. M. Cetegen and W. Yu, "*In-Situ* Particle Temperature, Velocity, and Size Measurements in DC Arc Plasma Thermal Sprays," *J. Therm. Spray Technol.*, **8** [1] 57–67 (1999).

[6]J. R. Fincke, "Diagnostics and Sensor Development for Thermal Spray Technologies"; pp. 1–9 in *Thermal Spray: International Advances in Coating Technology*. Edited by C. C. Berndt. ASM International, Materials Park, OH, 1992.

[7]L. Leblanc, C. Moreau, P. Gougeon, and J. Xi, "Long Term Stability of Plasma Spraying: Study on the Evolution of the In-Flight Particle State, Coating Microstructure, Voltage and Acoustic Emission"; pp. 306–11 in *United Thermal Spray Conference—1999*. Edited by E. Lugscheider and P. A. Kammer. German Welding Society, Dusseldorf, Germany, 1999.

[8]E. Lugscheider, F. Ladru, H.-A. Crostack, G. Reuss, and T. Haubold, "On-Line Process Monitoring During Spraying of TTBCs by Acoustic Emission Analysis"; pp. 312–20 in *United Thermal Spray Conference—1999*. Edited by E. Lugscheider and P. A. Kammer. German Welding Society, Dusseldorf, Germany, 1999.

[9]J. Knuuttila, P. Saarenrinne, R. Hernberg, T. Lehtinen, and T. Mantyla, "*In-Situ* Measurement of Particle Concentration and Velocity Using a Non-intensified CCD Camera"; pp. 577–82 in *Thermal Spray: A United Forum for Scientific and Technological Advances.* Edited by C. C. Berndt. ASM International, Materials Park, OH, 1998.

[10]J. Zierhut, K. Landes, C. Waas, D. Kutscher, D. P. Heinrich, and W. Krommer, "*In-Situ* Diagnostik bei Verfahren des Thermischen Beschichtens—Particle Flux Imaging (*In-Situ* Diagnostic Related to the Process of Thermal Coating–Particle Flux Imaging (PFI))"; pp. 340–44 in *United Thermal Spray Conference—1999*. Edited by E. Lugscheider and P. A. Kammer. German Welding Society, Dusseldorf, Germany, 1999.

[11]M. L. Boulos, P. Fauchais, A. Vardelle, and E. Pfender, "Fundamentals of Plasma Particle Momentum and Heat Transfer"; pp. 3–60 in *Plasma Spraying: Theory and Applications*. Edited by R. Suryanarayanan. World Science Publishing, Singapore, 1993.

[12]A. Vardelle, P. Fauchais, B. Dussoubs, and N. J. Themelis, "Heat Generation and Particle Injection in a Thermal Plasma Torch," *Plasma Chemistry and Plasma Processing*, **18** [4] 551–74 (1998).

[13]L. Pouliot, J. Blain, and F. Nadeau, *DPV-2000 Reference Manual*. Tecnar Automation Ltd., St. Hubert, Quebec, Canada, 1999.

[14]L. Leblanc, P. Gougeon, and C. Moreau, "Investigation of the Long-Term Stability of Plasma Spraying by Monitoring Characteristics of the Sprayed Particles"; pp. 567–75 in *Thermal Spray: A United Forum for Scientific and Technological Advances.* Edited by C. C. Berndt. ASM International, Materials Park, OH, 1998.

[15]L. Leblanc, C. Moreau, J.-G. Legoux, and B. Arsenault, "Characterization of Plasma Spray Processes by Monitoring the State of the Sprayed Particles"; pp. 329–34 in *United Thermal Spray Conference—1999.* Edited by E. Lugscheider and P. A. Kammer. German Welding Society, Dusseldorf, Germany, 1999.

[16]C. Moreau, P. Gougeon, A. Burgess, and D. Ross, "Characterization of Particle Flows in an Axial Injection Plasma Torch"; pp. 141–47 in *Advances in Thermal Spray Science and Technology*. Edited by C. C. Berndt and S. Sampath. ASM International, Materials Park, OH, 1995.

[17]M. Prystay, P. Gougeon, and C. Moreau, "Correlation Between Particle Temperature and Velocity and the Structure of Plasma Sprayed Zirconia Coatings"; pp. 517–23 in *Thermal Spray: Practical Solutions for Engineering Problems*. Edited by C. C. Berndt. ASM International, Materials Park, OH, 1996.

[18]A. Kucuk, R. S. Lima, and C. C. Berndt, "Influence of Plasma Spray Parameters on Formation and Morphology of $ZrO_2$–8 wt% $Y_2O_3$ Deposits," *J. Am. Ceram. Soc.*, **84** [4] 693–700 (2001).

[19]M. Leylavergne, B. Dussoubs, A. Vardelle, and N. Goubot, "Comparison of Plasma-Sprayed Coatings Produced in Argon or Nitrogen Atmosphere," *J. Therm. Spray Technol.*, **7** [4] 527–36 (1998).

[20]P. Fauchais, J. F. Coudert, M. Vardelle, A. Vardelle, and A. Denoirjean, "Diagnostics of Thermal Spraying Plasma Jets"; pp. 61–92 in *Plasma Spraying: Theory and Applications*. Edited by R. Suryanarayanan. World Science Publishing, Singapore, 1993.

[21]Y. A. Chivel, E. A. Kostyukevich, L. Y. Min'ko, V. S. Ivashko, V. A. Okovityj, and V. V. Kletsko, "Optical Diagnostics of Heterogeneous Gas-Flame and Plasma Jets"; pp. 527–29 in *United Thermal Spray Conference—1999*. Edited by E. Lugscheider and P. A. Kammer. German Welding Society, Dusseldorf, Germany, 1999.

[22]J. R. Fincke, W. D. Swank, and D. C. Haggard, "Inflight Behavior of Dissimilar Co-injected Particles in the Spraying of Metal–Ceramic Functionally Gradient Materials"; pp. 527–34 in *Thermal Spray: A United Forum for Scientific and Technological Advances.* Edited by C. C. Berndt. ASM International, Materials Park, OH, 1998.

[23]J. M. Leger, P. Fauchais, M. Grimaud, M. Vardelle, A. Vardelle, and B. Pateyron, "A New Ternary Mixture to Improve the Properties of Plasma Sprayed Ceramic Coatings"; pp. 17–20 in *Thermal Spray: International Advances in Coating Technology*. Edited by C. C. Berndt. ASM International, Materials Park, OH, 1992.

[24]J. R. Fincke, W. D. Swank, and D. C. Haggard, "The Influence of Injection Geometry and Carrier Gas Flow Rate on Spray Pattern"; pp. 335–42 in *Thermal Spray: A United Forum for Scientific and Technological Advances.* Edited by C. C. Berndt. ASM International, Materials Park, OH, 1998.

[25]M. Vardelle; Ph.D. Thesis. University of Limoges, Limoges, France, 1988 (as cited in Ref. 11).

[26]P. Eichert, M. Imbert, and C. Coddet, "Numerical Study of an Ar–$H_2$ Gas Mixture Flowing Inside and Outside a dc Plasma Torch," *J. Therm. Spray Technol.*, **7** [4] 505–12 (1998).

[27]J. R. Fincke and W. D. Swank, "Air-Plasma Spraying of Zirconia: Spray Characteristics and Standoff Distance Effect on Deposition Efficiency and Porosity"; pp. 513–18 in *Thermal Spray: International Advances in Coating Technology*. Edited by C. C. Berndt. ASM International, Materials Park, OH, 1992.

[28]A. Vardelle, M. Vardelle, P. Fauchais, P. Proulx, and M. I. Boulos, "Loading Effect by Oxide Powders in DC Plasma Jets"; pp. 543–47 in *Thermal Spray: International Advances in Coating Technology*. Edited by C. C. Berndt. ASM International, Materials Park, OH, 1992. □